Dynamics of Excited State Proton Transfer in Nitro Substituted 10-Hydroxybenzo[h]quinolines

Marciak, H.; Hristova, S.; Deneva, V; Kamounah, Fadhil S.; Hansen, Poul Erik; Lochbrunner, S; Antonov, Liudmil

Published in:
Physical Chemistry Chemical Physics

DOI:
10.1039/C7CP04476C

Publication date:
2017

Document Version
Peer reviewed version

Citation for published version (APA):
Marciak, H., Hristova, S., Deneva, V., Kamounah, F. S., Hansen, P. E., Lochbrunner, S., & Antonov, L. (2017). Dynamics of Excited State Proton Transfer in Nitro Substituted 10-Hydroxybenzo[h]quinolines. *Physical Chemistry Chemical Physics*, *19*(39), 26621-26629. https://doi.org/10.1039/C7CP04476C

Dynamics of Excited State Proton Transfer in Nitro Substituted 10-Hydroxybenzo[h]quinolines

H. Marciniak[1,2], S. Hristova[3], V. Deneva[3], F.S. Kamounah[4,5], P.E. Hansen[5], S. Lochbrunner[1], and L. Antonov[3]

[1] Institut für Physik, Universität Rostock, Albert-Einstein-Straße 23-24, 18059 Rostock, Germany
[2] Institut für Organische Chemie, Universität Würzburg, Am Hubland, 97074 Würzburg, Germany
[3] Institute of Organic Chemistry with Centre of Phytochemistry, Bulgarian Academy of Sciences, Acad. G. Bonchev str., bldg. 9, 1113 Sofia, Bulgaria
[4] Department of Chemistry, University of Copenhagen, Universitetsparken 5, DK-2100 Copenhagen Ø, Denmark
[5] Roskilde University, Department of Science and Environment, DK-4000, Roskilde, Denmark

Abstract

The ground state tautomerism and excited state intramolecular proton transfer (ESIPT) of 10-hydroxybenzo[h]quinoline (HBQ) and its nitro derivatives, 7-nitrobenzo[h]quinolin-10-ol (**2**) and 7,9-dinitrobenzo[h]quinolin-10-ol (**3**), has been studied in acetonitrile by steady state as well as time dependent spectroscopy and quantum-chemical calculations. In addition to the enol form absorbance in the range 360-390 nm, the absorption spectra of **2** and **3** exhibit a red shifted band at ~450 nm. Chemometric data processing, based on individual bands decomposition, allowed to estimate the position of the ground state enol-keto tautomeric equilibrium (ΔG values of 1.03 and 0.62 kcal/mol respectively for **2** and **3**). The fluorescence stems from the enol form even if the keto form is optically excited as proven by the shape of the excitation spectra indicating that ESIPT takes place. The Stokes shift of the substituted compounds is substantially lower compared to HBQ, which follows from the fact that the substitution occurs in the formal cyclohexa-2,4-dienone moiety and leads to decrease of the HOMO level of the keto tautomer. The pump-probe experiments show that in the nitro substituted HBQs **2** and **3** ESIPT happens with a time constant of 0.89 ps and 0.68 ps, respectively. In both cases a mixture of the enol and proton transfer form is optically excited. The enol form exhibits then the ESIPT and subsequently both fractions take the same relaxation path. We propose that in **2** and **3** the ESIPT path exhibits a potential energy barrier resulting in an incoherent rate governed process while in HBQ the ESIPT proceeds as a ballistic wavepacket motion along a path without significant barrier. The theoretical calculations (M06-2X/TZVP) confirm the existence of a barrier in the ground and excited state as result of the substitution.

Keywords: Proton transfer, excited state, ultrafast spectroscopy, 10-hydroxybenzo[h]quinoline

1. Introduction

The dynamics of hydrogen atoms and in particular of those involved in hydrogen bonds is a fundamental issue in chemistry and molecular biology. It is essential for the chemistry of acids and bases and crucial for isomeric and in particular tautomeric reactions. In addition, substances exhibiting intramolecular proton transfer in the excited as well as in the ground state have a large application potential in many different fields, e.g. as dyes, protecting substances against ultraviolet (UV) radiation and fast switches. Inter- and intramolecular proton transfer are, therefore, extensively investigated.[1] A broad class of molecules that contain an H-chelate ring exhibit typically fast excited state intramolecular proton transfer (ESIPT). [2–6] In the enol form of such compounds the hydrogen atom is bound to an oxygen and participating on a hydrogen bond to an acceptor atom at the opposite side of the chelate ring. After optical excitation the hydrogen atom is transferred to the acceptor atom and the keto isomer is formed in the electronically excited state. It was found that the transfer proceeds in many cases as a ballistic wavepacket motion along a nuclear coordinate involving the molecular backbone.[7–9] The wavepacket motion results in a transient contraction of the chelate ring which shifts the proton towards the acceptor. The bonds are changed from the enol to the keto configuration during the phase with the shortest donor-acceptor distance.[10] Depending on the effective mass of the moving moieties and the stiffness of the molecular skeleton transfer times between 30 fs and 100 fs have been observed.

10-hydroxybenzo[h]quinoline (HBQ, compound **1**, Scheme 1) is also a compound with an H-chelate ring. Ultrafast absorption measurements showed that due to the stiff backbone consisting of three condensed aromatic rings it exhibits an ESIPT processes which is very fast and takes only about 30-40 fs.[11,12] The findings rise the question if the reaction path is in all cases barrierless or if other situations can also occur and the barrier can be adjusted by suitable substitutions. Here we investigate substituted HBQs in which in one or two nitro groups are added to HBQ at the hydroxybenzo moiety resulting in p-NO_2 substituted HBQ (**2**) and o,p-dinitro substituted HBQ (**3**) respectively. The substitution results in a stabilization of the proton transfer form. While one would expect an even more downwards tilted reaction path for the ESIPT we show by time resolved pump-probe spectroscopy that on the contrary a barrier exists along the path.

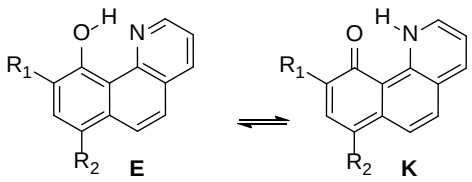

1: $R_1 = R_2 = H$
2: $R_1 = H$; $R_2 = NO_2$
3: $R_1 = R_2 = NO_2$

Scheme 1. HBQ and nitro substituted compounds.

2. Experimental Methods

Sample preparation:
The title compounds are synthesized and purified according to the already described procedures.[13,14] They are dissolved with a concentration in the order of 10^{-4} M in acetonitrile of Uvasol quality (Merck). Fused silica cuvettes with a thickness of 1 mm are employed as sample cells.

Steady-state absorption spectra:
The steady state UV/Vis absorption and emission spectra of the samples were recorded at room temperature by means of a Jasco V570 UV-Vis-NIR spectrophotometer and a Jasco FP6600 fluorimeter (both JASCO Inc, Japan). The exact positions of the bands were estimated by using derivative spectra calculated according to the "step-by-step filter" procedure.[15] The absorption spectra of **2** and **3** were analyzed by a quantitative procedure based on a decomposition of the overlapping bands, which yields the tautomeric molar fractions and the absorption spectra of the individual tautomers.[16,17] Quantum yields were calculated from a comparison with the fluorescence intensity of a solution of quinine in 1 M H_2SO_4.

NMR spectra:

All NMR spectra were measured by a Bruker 400 MHz Avance – III HD NMR spectrometer and analyzed with the software Topspin. As solvent acetonitrile-d_3 was used, which served also as a reference. All samples were measured at 25°C.

Time-dependent absorption measurements:

Femtosecond transient absorption measurements were performed by a pump-probe setup based on a non-collinear optical parametric amplifier (NOPA) for the generation of the excitation pulses and a white light continuum for probing.[18] To pump the NOPA and the white light stage a regenerative Ti:sapphire amplifier laser (CPA 2001, Clark MRX) system is used which provides at a repetition rate of 1 kHz energetic pulses with a center wavelength of 788 nm and a duration of 150 fs. To obtain excitation pulses at 305 nm the output of the NOPA is compressed by a sequence of fused silica prisms and then frequency doubled by a 100 µm thick BBO crystal.[19] The white light continuum used for probing is generated in a 4 mm thick calcium fluoride disc by focusing a fraction of a few microjoules of the Ti:sapphire output into the disc. The pump and probe beams are focused onto the sample to overlapping spots with diameters of about 200 µm and 100 µm, respectively. After the sample the probe beam is re-collimated and then spectrally dispersed by a prism and detected by a photodiode array with 512 pixels. The chirp of the probe light is corrected numerically. The energy of the excitation pulses is 500 nJ. Their polarization is set to the magic angle with respect to the probe polarization by an achromatic λ/2-plate to preclude that orientational relaxation contributes to the dynamics.

Theoretical calculations:

Quantum-chemical calculations were performed using the Gaussian 09 D.01 program suite.[20] If not otherwise specified, the M06-2X functional[21,22] was used with the TZVP basis set for the calculations in ground and excited state.[23] This fitted hybrid meta-GGA functional with 54% HF exchange was especially developed to describe main-group thermochemistry and non-covalent interactions. It shows very good results in predicting the position of tautomeric equilibria for compounds with intramolecular hydrogen bonds.[14,24–27] For comparison some additional functionals as implemented in Gaussian 09 D.01 (B3LYP[28], MN12SX[29], BHandH[30]) were used as well. Second and higher order Møller-Plesset perturbation theory (MP2-4)[31] and coupled-cluster theory with single, double, and perturbative triple excitations (CCSD(T)) [32] were used in addition for calculations of the ground state. The results for the relative stabilities of the tautomers of **2** and **3** in the ground and, in some cases, in the excited state are collected in Table S1 (Supplementary Information)., They justify the use of M06-2X/TZVP for the theoretical description of the ESIPT processes in this particular case.

The solvent effect of acetonitrile was described using the Polarizable Continuum Model (the integral equation formalism variant, IEFPCM, as implemented in Gaussian 09).[33] All ground state structures were optimized without restrictions, using tight optimization criteria and an ultrafine grid in the computation of two-electron integrals and their derivatives. The TD-DFT method[34–36], carried out with the same functional and basis set, was used for singlet excited state optimizations again without restrictions using normal optimization criteria and an ultrafine grid in the computation of two-electron integrals and their derivatives. The true minima were verified by performing frequency calculations in the corresponding environment. The emission spectra of the compounds were predicted using the procedure implemented in Gaussian 09 D.01.[20]

The transition states were estimated using the STQN method[37] and again verified by performing frequency calculations in the corresponding environment.

Vibrationally resolved electronic spectra were predicted using a recently developed procedure based on Franck-Condon analysis,[38–42] as it is implemented in Gaussian 09 D.01.[20] The subbands were described by using a Gaussian spectral function with a half-width at half-maximum of 500 cm^{-1}. The band positions in both compounds (**2** and **3**) were scaled by 0.1019 eV and 0.0876 eV (InpDEner keyword) for the absorption and emission spectra, respectively. In Figure S1 (Supplementary Information) the predicted absorption spectrum of the keto form of **2** is compared with the pure **2K** spectrum obtained by the band

decomposition technique. As can be seen the shape of the predicted spectrum agrees very well with the shape of the long-wavelength part of the experimentally determined absorption band of **2K**.

3. Results and Discussion

Steady State Absorption and Emission

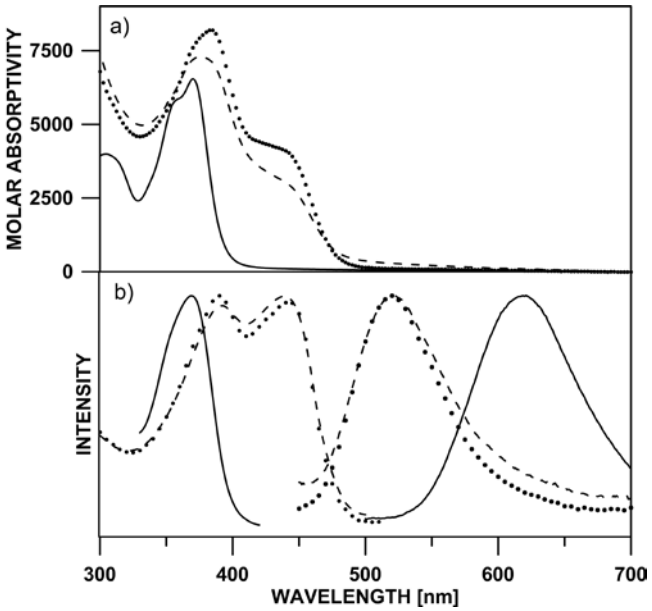

Figure 1. UV/Vis absorption (a), emission (b, right) and excitation (b, left) spectra of **1** (solid line), **2** (dashes) and **3** (dots) dissolved in acetonitrile.

Figure 1 shows the steady state absorption spectra of the three investigated compounds dissolved in acetonitrile. The nitro substituted compounds **2** and **3** exhibit in comparison to HBQ an additional low energy band around 440 nm (with a maximum at 447 nm as determined by second derivative spectroscopy) which extends their spectra into the visible. This absorption band is assigned to the proton transfer form (**K**) while the characteristic band between 350 nm and 390 nm observed for all three compounds is attributed to the enol form (**E**). The assignment is based on the fact that the fluorescence of HBQ which results from the excited state proton transfer form has a very strong Stokes shift (~ 11 000 cm^{-1}) with respect to the latter band (Figure 1b). According to the data from the literature it remains unclear if the availability of the keto tautomer in the ground state of **2** and **3** is a special feature of the nitro substituent(s). The spectral properties of substituted HBQs are usually reported for nonpolar solvents,[43] which makes the comparison difficult, because no keto absorption is observed for **2** and **3** in some of them.[14] However, analogues of **2** and **3** in which the nitro group(s) are replaced by CN group(s) do not show an absorption band around 440 nm in ethyl acetate[44], while the keto form is clearly seen in the same solvent in the case of **2** and **3**[14]. Compounds **2** and **3** have previously been investigated by NMR in DMF-d_7 and it was found that **3** existed to a large extent in the proton transfer form. In the deuterated compound deuterium isotope effects were observed for the hydrogen atoms H-2, H-3, H-4 and H-6. In a less polar solvent mixture of chlorform-d and tetrahydrofuran-d_4 (1:2) the amount of the proton transfer form was reduced considerably as judged from the coupling constant of NH with H-2[13]. In DMF-d_7 it was found to be 5.1 Hz, whereas it was reduced to 1.6 Hz in chlorform-d and tetrahydrofuran-d_4 suggesting an approximate content of the keto form of 30%. For **2** in DMF-d_7 similar deuterium isotope effects were observed suggesting that **2** is also to some extent on the proton transfer form. In the present investigation NMR spectra of **2** and **3** were recorded with acetonitrile-d_3 as solvent. The ^{1}H spectrum of **3** corresponds very much to that of **3** in a mixture of chloroform-d and tetrahydrofuran-d_4 (1:2) suggesting a content of the proton transfer form of 30%. For **2** the ^{1}H and ^{13}C NMR spectra are similar to those in DMF-d_7. This corresponds well to the results from the chemometric

processing of the steady-state absorption spectra, according to which the estimated amount of the keto tautomer is 15% in **2** and 26% in **3**, which corresponds to ΔG values of 1.03 and 0.62 kcal/mol, respectively.[14]

As seen from Figure 1, the emission spectra of **2** and **3** are independent in shape on the excitation (enol or keto maximum) and the Stokes shifts are lower (~ 7 000 cm^{-1} with respect to the maximum of the enol form). Both compounds exist obviously in the enol as well as in the proton transfer form while HBQ adopts only the enol form. The absorption spectrum of the keto form is red shifted with respect the enol absorption but contributes also at the absorption maximum of the enol tautomer. This is illustrated in Figure S1 (Supplementary information), where the individual spectra of **2** obtained by band decomposition are shown. The quantum yields of **1**-**3** determined with excitation at the absorption maximum of the enol form are 0.031, 0.018, and 0.028, while an excitation at the maximum of the keto tautomer gives 0.044 and 0.057 for **2** and **3**, respectively. The fluorescence spectrum is for all excitation wavelengths characteristic for the keto form indicating that the excited enol tautomer relaxes to the electronically excited state of the keto form before substantial fluorescence occurs. This notion is also in agreement with the pump-probe measurements discussed below. Assuming that all optically excited enol molecules relax quickly to the excited keto state the fluorescence yield is determined by the excited state lifetime of the keto form and it is independent on whether the enol or the keto form is excited. However, different yields are observed for different excitation wavelengths. One explanation might be that the yield can depend on the excess energy in the electronically excited state as it was observed for the proton transfer compound o-hydroxybenzaldehyde.[45] It might be the reason why the yields for exciting at the enol or keto maximum are different. Another possibility is that a relaxation channel from the electronically excited enol state directly back to the electronic ground state exists. In this case a branching in the early phase of the dynamics occurs and only a portion of the optically excited enol molecules performs proton transfer and reaches the excited keto state. Assuming that the fluorescence yield of the keto tautomer is independent on the excess energy one can estimate the yield of the enol form and the fraction experiencing proton transfer. In case of compound **2** we estimate from the decomposition of the absorption spectrum (see Fig. S1) that **2K** contributes with about 26% to the absorption at the enol maximum. The fluorescence yield *EY* of excited enol molecules can be calculated from the keto yield $KY = 0.044$ and the total yield $Y = 0.018$ for excitation at the enol maximum via $EY = (Y - 0.26 \cdot KY)/(1 - 0.26)$ resulting in an enol yield of $EY = 0.009$. If the lower yield after exciting the enol form is caused by an internal conversion path to the electronic ground state parallel to the excited state proton transfer the fraction of molecules performing proton transfer can be estimated from the ratio of the yields $EY/KY = 0.20$. The corresponding evaluations for compound **3** result in an enol yield of 0.021 and a proton transfer contribution of 0.37. Right now we cannot decide whether a reduction of the fluorescence yield with excess energy or an internal conversion in the enol configuration are responsible for the different fluorescence yields measured for excitation at the maximum of the enol and the keto absorption.

Pump-Probe Spectroscopy

Figure 2 shows for all three compounds, dissolved in acetonitrile, transient absorption spectra and corresponding time traces recorded by pump-probe spectroscopy with an optical excitation at 305 nm. In the case of HBQ the transient absorption is characterized by an excited state absorption (ESA) in the region between 380 nm and 560 nm and a negative contribution above 580 nm which is caused by stimulated emission (SE) from the electronically excited proton transfer form. Both signatures have appeared after the pump-probe correlation of 150 fs and exhibit only small changes in their spectral shape until they decay simultaneously on a timescale of few hundred picoseconds. These findings are in line with previous investigations which found a transfer time of 30-40 fs for the ESIPT and the associated rise of the stimulated emission and a return to the electronic ground state within 290 ps.[11]

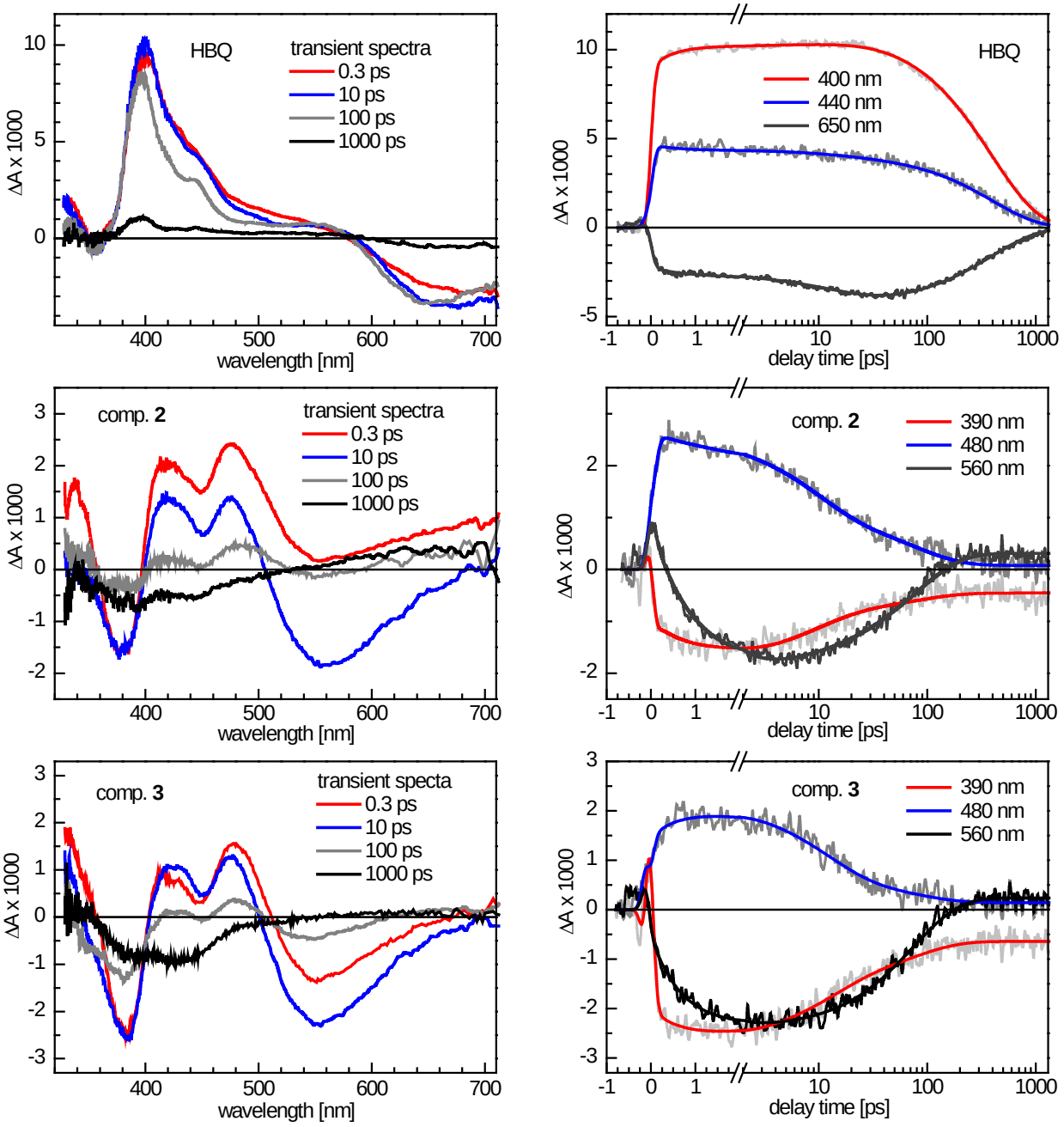

Figure 2. Transient absorption spectra at selected delay times after excitation (left column) and selected time traces (right column) of **1** (top row), **2** (middle row), and **3** (lower row) dissolved in acetonitrile. Fitted kinetics are shown in the right graphs as colored solid lines.

In the case of **2** and **3** the evolution of the transient absorption differs from HBQ. The spectra exhibit ESA roughly between 400 nm and 500 nm and show at longer wavelengths also a strong negative band due to stimulated emission from the electronically excited proton transfer form. However, this band grows in after the cross correlation on a sub-ps timescale indicating that the ESIPT is significantly slower than in **1**. Thereafter, most of the population returns to the ground state on a sub-100 ps time scale. At later times some residual long living bleach signal is observed at wavelengths shorter than 500 nm. It indicates that not all of the excited molecules return to the original ground state within the time window covered by the experiment. However, no accumulation of a signal and no sample degradation are observed. This shows that the sample recovers between the successive laser pulses which are separated by 1 ms. The nature of the long living state adapted by some of the molecules is not yet clear but might be a triplet state. It is interesting to note that the negative absorption change around 390 nm is during the first few picoseconds pretty stable. In this spectral region the bleach of the enol form dominates. It seems not to recover on the

sub-ps timescale, even not partially. This might indicate that no fast internal conversion path from the excited enol to the electronic ground state exists which can compete with the ESIPT. Accordingly, the variation of the fluorescence quantum yield with the excitation wavelength, which was discussed above, results probably from a reduction with excess energy in the keto form.

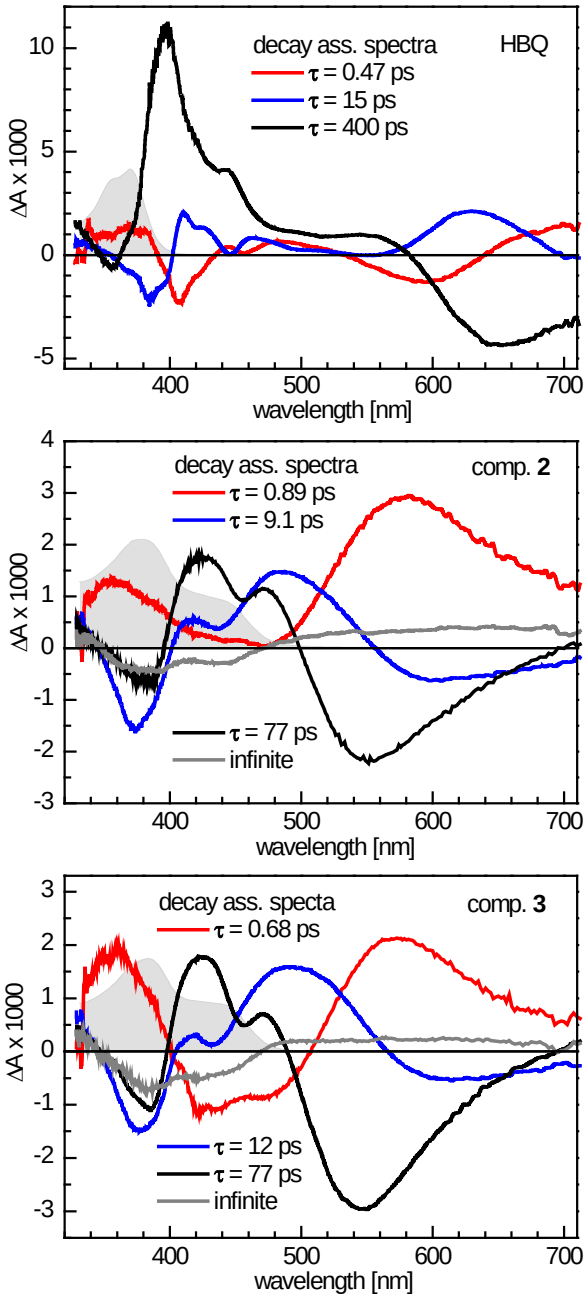

Figure 3. Decay associated spectra (DAS) resulting from global fits to the transient absorption spectra of HBQ (top), **2** (middle), and **3** (bottom). The fit function consists of three exponential decay components in the case of HBQ and of three exponential and a long living contribution for **2** (middle) and **3**. The obtained values for the decay times are given in the corresponding legends. The scaled stationary absorption spectra are shown as gray areas for comparison.

For a more detailed analysis and to determine the time of the proton transfer in **2** and **3** the model function $F(\lambda, t) = \sum_{i=1}^{3} DAS_i(\lambda) \cdot \exp(-t/\tau_i) + DAS_\infty(\lambda)$, convoluted with a Gaussian cross correlation to account for the time resolution of the experiment, was globally fitted to the measured pump-probe spectra of the three compounds. λ is the probe wavelength and t the delay time. τ_i represent exponential decay times and DAS_i decay associated spectra (DASs) which reflect the spectral shape of the corresponding

exponential component. DAS_∞ is a residual, long living contribution which has to be included in the case of compounds **2** and **3** while it was not necessary for **1**. The respective number of fit components is the minimal number to obtain satisfactory agreement between measurements and fits. The colored lines in the right column of Figure 2 represent fit results for the shown time traces demonstrating that good agreement between fit and data was achieved. Figure 3 shows the obtained DASs with the results for the fitted decay times given in the legends.

In the case of HBQ the dominant component describes the decay of the ESA and the stimulated emission and thereby the return to the ground state with a time constant of 400 ps. Previously a time of 290 ps was found for this process.[11] The difference results most probably from the fact that in the present measurements HBQ is dissolved in acetonitrile while in the former work cyclohexane was used as solvent. The DASs of the faster and subordinate contributions with time constants of 0.47 ps and 15 ps are smaller in amplitude and their spectral shapes correlate with the slope of the dominant component (see Fig. 3). This indicates that they reflect spectral shifts of the ESA and SE band and may be also a narrowing. We assign the 0.47 ps component to intramolecular vibrational energy redistribution (IVR) from optically excited modes and modes contributing to the ESIPT to all vibrational degrees of freedom of the molecule. This process occurs typically on a time scale of a few hundred femtoseconds and should be associated with some reshaping of the absorption spectrum. The 15 ps component reflects most probably cooling of the molecule by the solvent. The excess energy of about 2 eV which is the energy difference between the absorbed photon and the energy of the electronically excited proton transfer form is thereby dissipated into the solvent environment. This results typically in a blue shift and narrowing of the absorption bands as it is observed. In summary the two faster components reflect only redistribution of vibrational energy while the 400 ps component results from the relaxation of the electronically excited keto form to the electronic ground state.

In the case of **2** and **3** the fastest component with a time constant of 0.89 ps respective 0.68 ps is associated with changes in the ESA and a build-up of the proton transfer emission. Particularly the latter signature is a clear indicator for the ESIPT process. We therefore conclude that the ESIPT proceeds with a rate of $(0.89\ ps)^{-1}$ and $(0.68\ ps)^{-1}$, respectively in **2** and **3**. The DASs of the exponential components with 9.1 ps and 12 ps correlate in the green and red spectral region strongly with the slope of the SE and describe a blue shift of this band. We assign these components therefore to cooling of the molecules. However, this process is for the proton transfer dynamics of minor relevance. The slowest component, which has a time constant of 77 ps in both cases, reflects a decay of the overall signal and is ascribed to the depopulation of the electronically excited proton transfer state. Finally, some absorption changes remain for times longer than the window covered by the measurements. They consist of a bleach contribution at wavelengths below 480 nm and a weak and very broad ESA band at longer wavelengths. As already discussed a small fraction of the excited molecules seems not to return to the ground state within the 77 ps. However, the corresponding channel is also reversible and the molecules come back to the original ground state before the next laser pulse. Otherwise an accumulating signal and sample degradation would be observed contrary to our findings.

In summary, the experimental results show that in nitro substituted HBQs **2** and **3** ESIPT happens with a time constant of 0.89 ps respectively 0.68 ps. In both cases a mixture of the enol and proton transfer form is optically excited. The enol form exhibits then the ESIPT and subsequently both fractions take the same relaxation path. We propose that in **2** and **3** the ESIPT path exhibits a potential energy barrier resulting in an incoherent rate governed process and a sub-ps proton transfer time while in HBQ the ESIPT proceeds as ballistic wavepacket motion along a path without significant barrier.

Theoretical calculations

Both steady state and time dependent measurements clearly indicate a change in the spectroscopic behavior from **1** to **2**-**3** as a result of the nitro substitution. The available experimental information about the molar fractions of the tautomers in the ground state (ΔG values) and the information about the mechanism of the ESIPT allows to explain the observed variation in the spectroscopy of the compounds and

to verify the theoretical calculations. The energetics is sketched in Figure 4 and summarized in Table 1. As already discussed, HBQ exists only as enol tautomer in the ground and as keto form in the excited state.

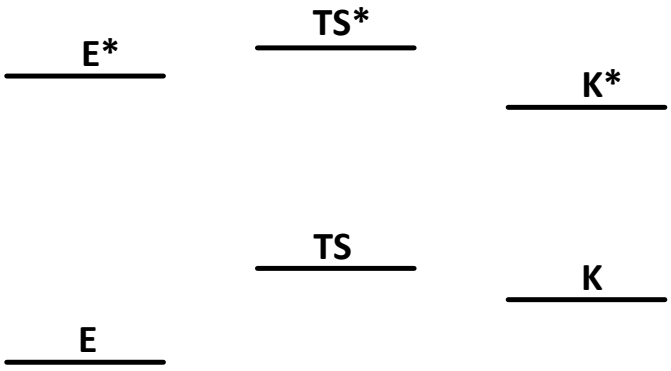

Figure 4. Sketch of the energetics of the proton transfer states for the studied compounds **2** and **3**. The corresponding values are compiled in Table 1.

Comparison of the data for **1** and **3** shows a different PT behavior. In **1** the proton transfer is barrierless in both ground and exited state as concluded from the extremely fast transfer dynamics. In contrast, the ground and excited state PT in **3** exhibits a potential energy barrier as shown by the pump probe experiments and the theoretical calculations. It is worth noticing that in all studied compounds the transfer of the proton is not a simple change of the OH distance, but accompanied by a variation in the N-O distance. As seen from Table 1 the shortest N-O distance is obtained at the transition states. Although not shown in the Table, according to the potential energy surface analysis, in HBQ the proton is exchanged at a N-O distance of ~2.4 Å (R_{OH}~1.3 Å) in the ground state and of ~2.39 Å (R_{OH}~1.25 Å) in the excited state. The differences between ground and excited state are not so pronounced, possibly due to the more rigid structure, which was interpreted as an indication for a partially proton-active mechanism where the movement of the proton itself plays a role in the process[11,12,46,47].

Table 1. Relative energies (in kcal/mol) of the forms of **1**-**3** in the ground and excited state along with the OH, NH, and NO distances (in Å) according to theoretical calculations (M06-2X/TZVP in acetonitrile).

Comp.	Ground state					Excited state				
	form	ΔE	O-H	N-H	N-O	form	ΔE	O-H	N-H	N-O
1	**E**	0.0	0.995	1.687	2.588	**K***	0.0	1.839	1.018	2.653
2	**E**	0.00	1.007	1.622	2.539	**E***	0.00	1.028	1.579	2.521
	TS	4.96	1.379	1.137	2.429	**TS***	1.30	1.204	1.282	2.416
	K	4.86	1.526	1.075	2.483	**K***	3.03	1.797	1.021	2.616
3	**E**	0.00	1.029	1.538	2.490	**E***	1.36	1.025	1.563	2.504
	TS	1.89	1.257	1.213	2.398	**TS***	7.11	1.300	1.176	2.385
	K	0.58	1.615	1.048	2.517	**K***	0.00	1.810	1.020	2.614

As discussed by Chou at al.[44] the substituent effect on the enol tautomer is expected to be small in HBQ due to its aromaticity, which means the π–electrons are extensively delocalized leading to a simultaneous perturbation of both HOMO and LUMO levels. For this reason the absorption spectra of the enol tautomers of the substituted HBQs are quite similar to that of HBQ.[43,48] However, in the keto tautomer charge separation occurs and HOMO and LUMO are located at the cyclohexa-2,4-dienone and methylenepyridine

moiety, respectively. This leads to a different substituent effect. An electron accepting substituent at the cyclohexa-2,4-dienone part leads to a decrease of the HOMO level and correspondingly to an increase of the HOMO-LUMO gap and a blue shift of the emission. On the contrary, electron donating groups rise the energy of the HOMO level and cause a red shift of the emission. Substitution at the methylenepyridine influences correspondingly the LUMO energy causing a decrease of it if an electron acceptor is present. An opposite effect is expected for the case of adding an electron donating substituent. As can be seen from Figure 5 for compound **3** the HOMO and LUMO orbitals of the enol form are delocalized over the π-electron network, while in **3K** charge separation is evident in agreement with Chou at al.[44]As a consequence of attaching electron acceptor(s) at the cyclohexa-2,4-dienone part a strong blue shift of the emission of **2** and **3** compared to HBQ is observed. However, the effect, as seen in Figure 1, is not cumulative.

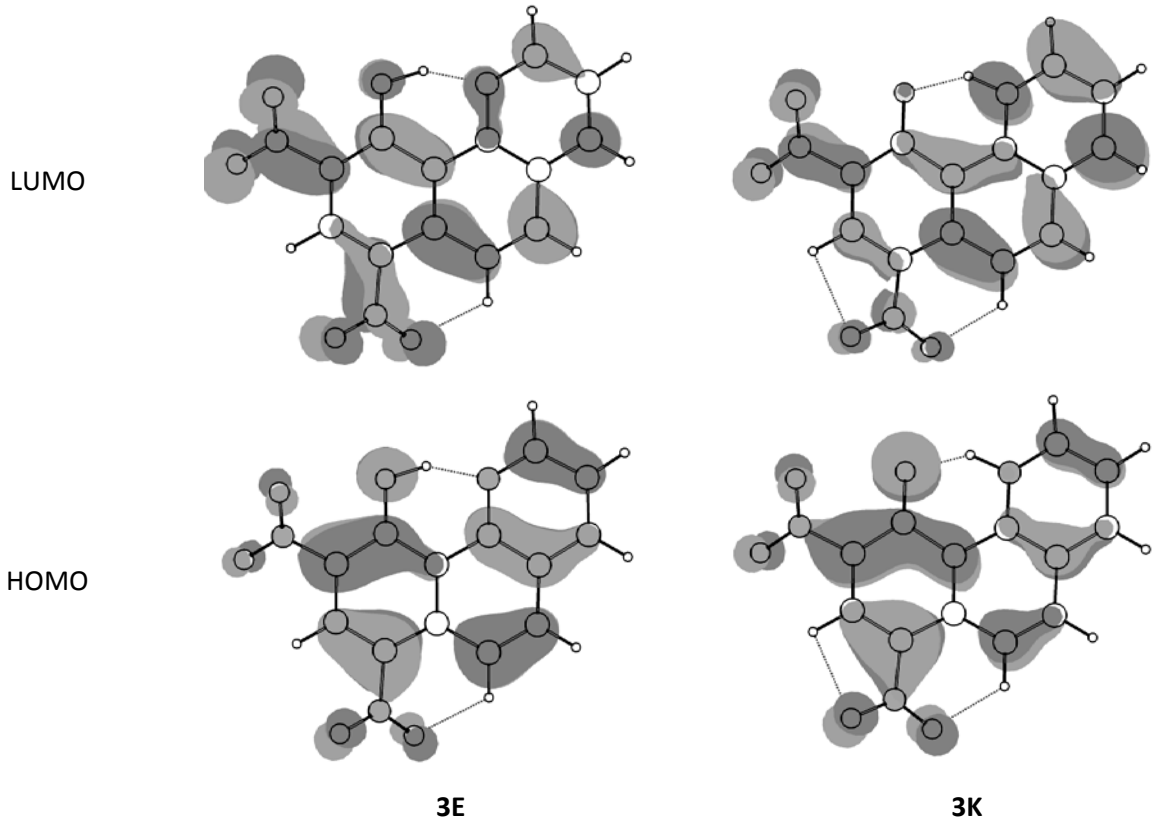

Figure 5. Frontier molecular orbitals in **3**.

4. Conclusions

The steady state and time dependent measurements of HBQ and its nitro substituted derivatives **2** and **3** in acetonitrile have shown that the substitution leads to the appearance of corresponding keto tautomers in the ground state and the ESIPT path exhibits a potential energy barrier. HBQ exists in S_0 only as enol tautomer and the ESIPT proceeds as ballistic wavepacket motion along a path without significant barrier. The spectral behavior of **2** and **3** is quite similar in the ground and excited state, i.e. no cumulative effect of the increased number of nitro groups is detected.

The experimentally obtained ΔG values for **2** and **3** allowed to verify the DFT calculations with respect to the correct prediction of the tautomerism of these compounds. The theoretical calculations using M06-2X/TZVP reproduce reasonably well the experimental results in the case of HBQ and **3**. In HBQ a barrierless proton transfer occurs, while stable enol and keto forms are available in both S_0 and S_1 of **3**. The calculations fail to describe the situation in **2,** overestimating the stability of the ground and excited state enol tautomers, but predict correctly that the PT proceeds over potential energy barriers.

The substitution does not affect substantially the absorption spectra of the enol tautomers due to the delocalization of the π–electrons. In the case of the keto form, where the HOMO and the LUMO levels are separated, the substitution with nitro group(s) at the cyclohexa-2,4-dienone part leads to a decrease of the HOMO level and to a blue shift of the emission spectra. The absorption spectra of the keto tautomers, constructed by applying band decomposition techniques, correspond in shape well to the theoretical potential energy curves according to a Frank-Condon analysis.

5. Acknowledgement

Financial support from Bulgarian National Science Fund (DCOST01/05/2017 project as well as access to MADARA computer cluster by the project RNF01/0110), CMST COST Action CM1405 MOLIM, Swiss National Science Foundation (SupraMedChem@Balkans.Net Institutional partnership project) and Alexander von Humboldt foundation (equipment donation) is gratefully acknowledged. We are grateful to Wolfgang Breitsprecher for his help with the sample preparation.

References

1 J. T. Hynes, J. P. Klinman, H.-H. Limbach and R. L. Schowen, Eds., *Hydrogen-Transfer Reactions*, Wiley-VCH Verlag GmbH & Co. KGaA, Weinheim, Germany, 2006.

2 T. Elsaesser, B. Schmetzer, M. Lipp and R. J. Bäuerle, Excited-state proton transfer in 2-(2′-hydroxyphenyl)benzothiazole: Transient electronic absorption measured on the picosecond time scale, *Chemical Physics Letters*, 1988, **148**, 112–118.

3 F. Laermer, T. Elsaesser and W. Kaiser, Femtosecond spectroscopy of excited-state proton transfer in 2-(2′-hydroxyphenyl)benzothiazole, *Chemical Physics Letters*, 1988, **148**, 119–124.

4 P. F. Barbara, P. K. Walsh and L. E. Brus, Picosecond kinetic and vibrationally resolved spectroscopic studies of intramolecular excited-state hydrogen atom transfer, *The Journal of Physical Chemistry*, 1989, **93**, 29–34.

5 A. Douhal, F. Lahmani and A. H. Zewail, Proton-transfer reaction dynamics, *Chemical Physics*, 1996, **207**, 477–498.

6 T. Kumpulainen, B. Lang, A. Rosspeintner and E. Vauthey, Ultrafast Elementary Photochemical Processes of Organic Molecules in Liquid Solution, *Chemical Reviews*, , DOI:10.1021/acs.chemrev.6b00491.

7 S. Lochbrunner, A. J. Wurzer and E. Riedle, Microscopic Mechanism of Ultrafast Excited-State Intramolecular Proton Transfer: A 30-fs Study of 2-(2′-Hydroxyphenyl)benzothiazole †, *The Journal of Physical Chemistry A*, 2003, **107**, 10580–10590.

8 S. Lochbrunner, C. Schriever and E. Riedle, in *Hydrogen-Transfer Reactions*, eds. J. T. Hynes, J. P. Klinman, H.-H. Limbach and R. L. Schowen, Wiley-VCH Verlag GmbH & Co. KGaA, Weinheim, Germany, 2006, pp. 349–375.

9 C. Schriever, S. Lochbrunner, A. R. Ofial and E. Riedle, The origin of ultrafast proton transfer: Multidimensional wave packet motion vs. tunneling, *Chemical Physics Letters*, 2011, **503**, 61–65.

10 G. A. Parada, T. F. Markle, S. D. Glover, L. Hammarström, S. Ott and B. Zietz, Control over Excited State Intramolecular Proton Transfer and Photoinduced Tautomerization: Influence of the Hydrogen-Bond Geometry, *Chemistry - A European Journal*, 2015, **21**, 6362–6366.

11 C. Schriever, M. Barbatti, K. Stock, A. J. A. Aquino, D. Tunega, S. Lochbrunner, E. Riedle, R. de Vivie-Riedle and H. Lischka, The interplay of skeletal deformations and ultrafast excited-state intramolecular proton transfer: Experimental and theoretical investigation of 10-hydroxybenzo[h]quinoline, *Chemical Physics*, 2008, **347**, 446–461.

12 J. Lee, C. H. Kim and T. Joo, Active Role of Proton in Excited State Intramolecular Proton Transfer Reaction, *The Journal of Physical Chemistry A*, 2013, **117**, 1400–1405.

13 P. E. Hansen, F. Kamounah and D. Gryko, Deuterium Isotope Effects on 13C-NMR Chemical Shifts of 10-Hydroxybenzo[h]quinolines, *Molecules*, 2013, **18**, 4544–4560.

14 S. Hristova, G. Dobrikov, F. S. Kamounah, S. Kawauchi, P. E. Hansen, V. Deneva, D. Nedeltcheva and L. Antonov, 10-Hydroxybenzo[h]quinoline: switching between single- and double-well proton transfer through structural modifications, *RSC Advances*, 2015, **5**, 102495–102507.

15 L. Antonov, Drawbacks of the present standards for processing absorption spectra recorded linearly as a function of wavelength, *TrAC Trends in Analytical Chemistry*, 1997, **16**, 536–543.

16 L. Antonov and D. Nedeltcheva, Resolution of overlapping UV–Vis absorption bands and quantitative analysis, *Chemical Society Reviews*, 2000, **29**, 217–227.

17 L. Antonov, in *Tautomerism: Methods and Theories*, ed. L. Antonov, Wiley-VCH, Weinheim, Germany, 2013, pp. 25–47.

18 E. Riedle, M. Beutter, S. Lochbrunner, J. Piel, S. Schenkl, S. Spörlein and W. Zinth, Generation of 10 to 50 fs pulses tunable through all of the visible and the NIR, *Applied Physics B*, 2000, **71**, 457–465.

19 P. Baum, S. Lochbrunner and E. Riedle, Generation of tunable 7-fs ultraviolet pulses: achromatic phase matching and chirp management, *Applied Physics B*, 2004, **79**, 1027–1032.

20 M. J. Frisch, G. W. Trucks, H. B. Schlegel, G. E. Scuseria, M. A. Robb, J. R. Cheeseman, G. Scalmani, V. Barone, B. Mennucci, G. A. Petersson, H. Nakatsuji, M. Caricato, X. Li, H. P. Hratchian, A. F. Izmaylov, J. Bloino, G. Zheng, J. L. Sonnenberg, M. Hada, M. Ehara, K. Toyota, R. Fukuda, J. Hasegawa, M. Ishida, T. Nakajima, Y. Honda, O. Kitao, H. Nakai, T. Vreven, J. A. Montgomery Jr., J. E. Peralta, F. Ogliaro, M. J. Bearpark, J. Heyd, E. N. Brothers, K. N. Kudin, V. N. Staroverov, R. Kobayashi, J. Normand, K. Raghavachari,

A. P. Rendell, J. C. Burant, S. S. Iyengar, J. Tomasi, M. Cossi, N. Rega, N. J. Millam, M. Klene, J. E. Knox, J. B. Cross, V. Bakken, C. Adamo, J. Jaramillo, R. Gomperts, R. E. Stratmann, O. Yazyev, A. J. Austin, R. Cammi, C. Pomelli, J. W. Ochterski, R. L. Martin, K. Morokuma, V. G. Zakrzewski, G. A. Voth, P. Salvador, J. J. Dannenberg, S. Dapprich, A. D. Daniels, Ã. Farkas, J. B. Foresman, J. V. Ortiz, J. Cioslowski and D. J. Fox, *Gaussian 09 Revision D.01*, Gaussian, Inc., Wallingford, CT, USA, 2013.

21 Y. Zhao and D. G. Truhlar, Density Functionals with Broad Applicability in Chemistry, *Accounts of Chemical Research*, 2008, **41**, 157–167.

22 Y. Zhao and D. G. Truhlar, The M06 suite of density functionals for main group thermochemistry, thermochemical kinetics, noncovalent interactions, excited states, and transition elements: two new functionals and systematic testing of four M06-class functionals and 12 other functionals, *Theoretical Chemistry Accounts*, 2008, **120**, 215–241.

23 F. Weigend and R. Ahlrichs, Balanced basis sets of split valence, triple zeta valence and quadruple zeta valence quality for H to Rn: Design and assessment of accuracy, *Physical Chemistry Chemical Physics*, 2005, **7**, 3297.

24 Y. Manolova, V. Kurteva, L. Antonov, H. Marciniak, S. Lochbrunner, A. Crochet, K. M. Fromm, F. S. Kamounah and P. E. Hansen, 4-Hydroxy-1-naphthaldehydes: proton transfer or deprotonation, *Physical Chemistry Chemical Physics*, 2015, **17**, 10238–10249.

25 Y. Manolova, H. Marciniak, S. Tschierlei, F. Fennel, F. S. Kamounah, S. Lochbrunner and L. Antonov, Solvent control of intramolecular proton transfer: is 4-hydroxy-3-(piperidin-1-ylmethyl)-1-naphthaldehyde a proton crane?, *Physical Chemistry Chemical Physics*, 2017, **19**, 7316–7325.

26 Y. Manolova, V. Deneva, L. Antonov, E. Drakalska, D. Momekova and N. Lambov, The effect of the water on the curcumin tautomerism: A quantitative approach, *Spectrochimica Acta Part A: Molecular and Biomolecular Spectroscopy*, 2014, **132**, 815–820.

27 D. Ivanova, V. Deneva, D. Nedeltcheva, F. S. Kamounah, G. Gergov, P. E. Hansen, S. Kawauchi and L. Antonov, Tautomeric transformations of piroxicam in solution: a combined experimental and theoretical study, *RSC Advances*, 2015, **5**, 31852–31860.

28 A. D. Becke, Density-functional thermochemistry. III. The role of exact exchange, *The Journal of Chemical Physics*, 1993, **98**, 5648–5652.

29 R. Peverati and D. G. Truhlar, Screened-exchange density functionals with broad accuracy for chemistry and solid-state physics, *Physical Chemistry Chemical Physics*, 2012, **14**, 16187.

30 A. D. Becke, A new mixing of Hartree–Fock and local density-functional theories, *The Journal of Chemical Physics*, 1993, **98**, 1372–1377.

31 C. Møller and M. S. Plesset, Note on an Approximation Treatment for Many-Electron Systems, *Physical Review*, 1934, **46**, 618–622.

32 J. D. Watts, J. Gauss and R. J. Bartlett, Coupled-cluster methods with noniterative triple excitations for restricted open-shell Hartree–Fock and other general single determinant reference functions. Energies and analytical gradients, *The Journal of Chemical Physics*, 1993, **98**, 8718–8733.

33 J. Tomasi, B. Mennucci and R. Cammi, Quantum Mechanical Continuum Solvation Models, *Chemical Reviews*, 2005, **105**, 2999–3094.

34 R. Improta, in *Computational Strategies for Spectroscopy*, ed. V. Barone, John Wiley & Sons, Inc., Hoboken, NJ, USA, 2011, pp. 37–75.

35 C. Adamo and D. Jacquemin, The calculations of excited-state properties with Time-Dependent Density Functional Theory, *Chemical Society Reviews*, 2013, **42**, 845–856.

36 L. Antonov, S. Kawauchi and Y. Okuno, Prediction of the color of dyes by using time-dependent density functional theory, *Bulgarian Chemical Communications*, 2014, **46**, 228–237.

37 C. Peng, P. Y. Ayala, H. B. Schlegel and M. J. Frisch, Using redundant internal coordinates to optimize equilibrium geometries and transition states, *Journal of Computational Chemistry*, 1996, **17**, 49–56.

38 V. Barone, J. Bloino, M. Biczysko and F. Santoro, Fully Integrated Approach to Compute Vibrationally Resolved Optical Spectra: From Small Molecules to Macrosystems, *Journal of Chemical Theory and Computation*, 2009, **5**, 540–554.

39 A. Baiardi, J. Bloino and V. Barone, General Time Dependent Approach to Vibronic Spectroscopy Including Franck–Condon, Herzberg–Teller, and Duschinsky Effects, *Journal of Chemical Theory and Computation*, 2013, **9**, 4097–4115.
40 V. Barone, A. Baiardi, M. Biczysko, J. Bloino, C. Cappelli and F. Lipparini, Implementation and validation of a multi-purpose virtual spectrometer for large systems in complex environments, *Physical Chemistry Chemical Physics*, 2012, **14**, 12404.
41 V. Barone, The virtual multifrequency spectrometer: a new paradigm for spectroscopy: A new paradigm for spectroscopy, *Wiley Interdisciplinary Reviews: Computational Molecular Science*, 2016, **6**, 86–110.
42 J. Bloino, A. Baiardi and M. Biczysko, Aiming at an accurate prediction of vibrational and electronic spectra for medium-to-large molecules: An overview, *International Journal of Quantum Chemistry*, 2016, **116**, 1543–1574.
43 K.-Y. Chen, H.-Y. Tsai, W.-C. Lin, H.-H. Chu, Y.-C. Weng and C.-C. Chan, ESIPT fluorescent dyes with adjustable optical properties: Substituent and conjugation effects, *Journal of Luminescence*, 2014, **154**, 168–177.
44 K.-Y. Chen, C.-C. Hsieh, Y.-M. Cheng, C.-H. Lai and P.-T. Chou, Extensive spectral tuning of the proton transfer emission from 550 to 675 nm via a rational derivatization of 10-hydroxybenzo[h]quinoline, *Chemical Communications*, 2006, 4395.
45 K. Stock, T. Bizjak and S. Lochbrunner, Proton transfer and internal conversion of o-hydroxybenzaldehyde: coherent versus statistical excited-state dynamics, *Chemical Physics Letters*, 2002, **354**, 409–416.
46 M. Higashi and S. Saito, Direct Simulation of Excited-State Intramolecular Proton Transfer and Vibrational Coherence of 10-Hydroxybenzo[h]quinoline in Solution, *The Journal of Physical Chemistry Letters*, 2011, 2366–2371.
47 S. Takeuchi and T. Tahara, Coherent Nuclear Wavepacket Motions in Ultrafast Excited-State Intramolecular Proton Transfer:? Sub-30-fs Resolved Pump?Probe Absorption Spectroscopy of 10-Hydroxybenzo[h]quinoline in Solution, *The Journal of Physical Chemistry A*, 2005, **109**, 10199–10207.
48 J. Piechowska, K. Huttunen, Z. Wrubel, H. Lemmetyinen, N. V. Tkachenko and D. T. Gryko, Excited State Intramolecular Proton Transfer in Electron-Rich and Electron-Poor Derivatives of 10-Hydroxybenzo[*h*]quinoline, *The Journal of Physical Chemistry A*, 2012, **116**, 9614–9620.